



Published in final edited form as:

Comput Biol Med. 2020 February ; 117: 103620. doi:10.1016/j.combiomed.2020.103620.

Predicting abdominal aortic aneurysm growth using patient-oriented growth models with two-step Bayesian inference

Emrah Akkoyun¹, Sebastian T. Kwon², Aybar C. Acar¹, Whal Lee³, Seungik Baek^{4,*}

¹Department of Health Informatics, Graduate School of Informatics, Middle East Technical University, Dumlupinar Bulvari #1, 06800 Cankaya, Ankara, Turkey.

²Department of Anesthesiology and Perioperative Medicine, UCLA David Geffen School of Medicine, 757 Westwood Blvd., Los Angeles, CA 90095, USA.

³Department of Radiology, Seoul National University Hospital, 101 Daehangno, Jongno-gu, Seoul, Republic of Korea.

⁴Department of Mechanical Engineering, Michigan State University, 2457 Engineering Building, East Lansing, MI 48824, USA.

Abstract

Objective: For small abdominal aortic aneurysms (AAAs), a regular follow-up examination is recommended every 12 months for AAAs of 30–39 mm and every six months for AAAs of 40–55 mm. Follow-up diameters can determine if a patient follows the common growth model of the population. However, the rapid expansion of an AAA, often associated with higher rupture risk, may be overlooked even though it requires surgical intervention. Therefore, the prognosis of abdominal aortic aneurysm growth is clinically important for planning treatment. This study aims to build enhanced Bayesian inference methods to predict maximum aneurysm diameter.

Methods: 106 CT scans from 25 Korean AAA patients were retrospectively obtained. A two-step approach based on Bayesian calibration was used, and an exponential abdominal aortic aneurysm growth model (population-based) was specified according to each individual patient's growth (patient-specific) and morphologic characteristics of the aneurysm sac (enhanced). The distribution estimates were obtained using a Markov Chain Monte Carlo (MCMC) sampler.

*Address for Correspondence: S. Baek, Ph.D., Department of Mechanical Engineering, Michigan State University, 2457 Engineering Building, East Lansing, MI 48824, T: +1-517-432-3161, F: +1-517-353-1750, sbaek@egr.msu.edu.

Declaration of interests

The authors declare that they have no known competing financial interests or personal relationships that could have appeared to influence the work reported in this paper.

The authors declare the following financial interests/personal relationships which may be considered as potential competing interests:

Conflict of interest

No conflicts of interest are declared by the authors.

Publisher's Disclaimer: This is a PDF file of an unedited manuscript that has been accepted for publication. As a service to our customers we are providing this early version of the manuscript. The manuscript will undergo copyediting, typesetting, and review of the resulting proof before it is published in its final form. Please note that during the production process errors may be discovered which could affect the content, and all legal disclaimers that apply to the journal pertain.

Results: The follow-up diameters were predicted satisfactorily (i.e. the true follow-up diameter was in the 95% prediction interval) for 79% of the scans using the population-based growth model, and 83% of the scans using the patient-specific growth model. Among the evaluated geometric measurements, centerline tortuosity was a significant ($p=0.0002$) predictor of growth for AAAs with accelerated and stable expansion rates. Using the enhanced prediction model, 86% of follow-up scans were predicted satisfactorily. The average prediction errors of population-based, patient-specific, and enhanced models were ± 2.67 , ± 2.61 and ± 2.79 mm, respectively.

Conclusion: A computational framework using patient-oriented growth models provides useful tools for per-patient basis treatment and enables better prediction of AAA growth.

Keywords

Abdominal aortic aneurysm; probabilistic programming; Bayesian inference; rupture risk assessment; patient-oriented prediction model

1. INTRODUCTION

An Abdominal Aortic Aneurysm (AAA) is diagnosed by an enlargement of the abdominal aorta to 30 mm or more in diameter [1]. Rupture of the AAA, associated with over 80% mortality, may eventually be observed if no surgical intervention, either open surgery or Abdominal Endovascular Aneurysm Repair (EVAR) intervention is performed [2]. Decision-making related to clinical management for AAA patients is complex, because the evaluation of the rupture risk can only be assessed by monitoring the AAA without any intervention, which has its own risk. There have been several papers [3]–[6], wherein the traditional guideline for clinical AAA management based on a single criterion has been challenged; alternatives have been proposed which take into account various factors such as growth rate [3][6], AAA volume [4], thrombus accumulation [8], asymmetry and tortuosity [8][9] for improved assessment of aneurysm development and rupture risk. Particularly, there is recent consensus that the growth rate is critical for AAA clinical management even for small diameter AAAs [11]. Lee et al. [12] summarized responses from vascular surgeons stating that “discovering new tests to predict [that] an AAA will be fast growing” should be a top research priority.

Motivated by recent studies, this study aims to develop a tool that detects patients who have fast growing AAAs and predicts the growth rates of their respective aneurysms during surveillance. There has been substantial heterogeneity of AAA growth rates among various studies; some studies reported that 11.4% [3] and 12% [13] of AAAs stop expanding, while others reported that AAA diameter size was associated with increases of growth rate [7]. The difficulty of AAA growth rate prediction was exacerbated by the high uncertainty of different diameter measurements so Gharahi et al. [5] suggested an alternative, semi-automatic method of measuring the maximally inscribed spherical diameter, reducing uncertainty in measurements. Akkoyun et al. [14] then investigated the correlations among 21 geometrical measurements of retrospectively obtained longitudinal CT scan images and concluded that “spherical diameter” could be the most accurate predictor representative of the growth curve.

Even by minimizing the uncertainty of measurement, the variability of AAA expansion rates is still high [15]. It is unclear why some patients have AAAs with accelerated expansion rates, while others, with identical risk profiles, do not [16]. This makes prediction of the natural growth pattern difficult because aneurysm growth over time does not necessarily follow a common pattern [16][17]. Significant progress has been made toward patient-specific AAA growth modeling to assess the rupture risk using biological tissue growth and remodeling (G&R) [18][19]. Zeinali-Davarani et al. presented patient-specific modeling of an AAA, which is able to trace alterations of the geometry [19]. In summary, these G&R models used finite element method (FEM) to simulate the exact mechanical state of an AAA at a given time but do not accommodate the uncertainty in their predictions [20].

There is emerging evidence that the geometrical properties of an AAA might provide more valuable information for predicting AAA growth [21]. Shum et al. [22] derived 28 geometrical measurements from 76 CTA scans describing the size and shape of the aneurysm, and developed a model capable of discriminating aneurysms as ruptured and unruptured with an accuracy of 86.6%. Similarly, Parikh et al. [23] investigated geometrical indices derived from 75 electively and 75 emergently repaired AAA scans, and revealed the three most significant indices in the classification of an AAA (with an average accuracy of 81.0%) using decision trees, a machine learning algorithm. Similarly, Lee et al. [21] applied a non-linear support vector regression (SVR) model to predicting patient-oriented growth with an additional biomarker, flow mediated dilation. These tools can be categorized under supervised machine learning, yielding discrete categorical output (e.g. ruptured vs unruptured), and provide single maximum likelihood estimates. In contrast, the model in this study provides predictive distributions of the aneurysm growth with the associated uncertainty inherent in the distribution.

In this study, a two-step approach based on Bayesian calibration [24] was used and the aneurysm growth model was specified according to individual patient characteristics. The estimated distributions on samples were drawn from the specified model using Markov Chain Monte Carlo (MCMC) samplers [20]. This estimate is made practical by using automatic Bayesian inference on a user-defined probabilistic model, which sharpens the subjective prior belief in the probability of an event by incorporating experimental data [26] [27]. MCMC is used frequently for Bayesian inference [27]–[29]. However, to the best of our knowledge it has not been used before in AAA diameter estimation. The unique computational advantage of this approach, which is; incorporating prior belief (i.e. a generalized model) with observations (i.e. the scans) results in the prediction of diameters with associated uncertainty at any time-point and in the capability of taking individual characteristics and other geometry into account.

To this end, an exponential growth model was built specifically on patient characteristics using 21 geometrical measurements derived from 106 Computed Tomography (CT) scan images. Thus, the prediction of a measurement at any time-point can be made, along with an associated uncertainty to provide a clinically helpful tool for surgical planning and patient management during the surveillance of abdominal aortic aneurysms.

2. METHODS

2.1. CT Scan Data

We recently studied AAA geometric evolution using retrospective longitudinal CT images (Akkoyun et al., submitted). Specifically, 106 CT scans from 25 patients obtained from Seoul National University Hospital, South Korea, were used to construct 3D models of the aneurysms and calculate 21 different measurements describing the geometrical properties of the aneurysms. 3D medical imaging software, MIMICS (Materialise, Leuven, Belgium), was used to semi-automatically construct a 3D model of each aneurysm sac between the most inferior renal artery and iliac bifurcation region. Since the aneurysm sac has a complex and dynamic structure, a number of different measurements are required to reflect its complexity in different aspects and to properly observe the change over time. The list of all measurements and their definitions, which were introduced by Gharahi et al.[5], are summarized in Table 1. Volume measurements are denoted by VOL and the global maximum and minimum of local measurements are denoted by MAX and MIN, respectively.

Patients were monitored and scanned at various time intervals between 6 to 56 months with a median interval of 11 months. 81 of the 106 scans were used for diameter prediction, as the first scan of each patient (i.e. the baseline) is assumed to be known, and required, for the prediction of subsequent diameters. Therefore, one scan per patient (for a total of 25 scans) was excluded from the follow-up set, leaving 81. In addition to predicting the follow-up diameter at any arbitrary time, we also categorized the scans to time intervals of 6–18 and 18–30 months as 1st and 2nd year, respectively, to be able to compare the performance of the prediction models with other studies presented in literature, which use yearly time categories. Retrospective growth data were recorded at the 1st year (10±4 months) in 68 scans and at the 2nd year (20±3 months) in 8 scans. We did not categorize the remaining 5 scans, recorded after 30 months (44±13 months).

2.2. Exponential AAA Growth Model

Previous studies demonstrated that aneurysm growth should be modeled in a non-linear fashion [4], [5]. In this study, we consider an AAA growth model using the maximum spherical diameter, in which the diameter D at time t is given by

$$D(t) = \alpha e^{\beta t} \quad (1)$$

where α denotes the initial maximum diameter at $t = 0$ and β denotes the diameter growth rate. In the analytic solution approach, α and β are the parameters, each of which takes a constant value for a given data set.

2.3. Bayesian Framework of Model Calibrations

A Bayesian inference technique calibrates the growth model with clinical data and predicts future AAA growth for each patient. To test the prediction capability of AAA growth, the Quantity of Interest (QoI) is defined as the maximum spherical diameter expansion rate for per-patient and specific cases. That is, each time point that a CT scan obtained was

sequentially selected as a QoI, which enables us to determine a statistical model and investigate the associated uncertainties.

The scans were categorized into three classes: ‘over-estimated’, ‘under-estimated’ and ‘within tolerance’, based on whether the true follow-up diameter was below, above, or within the 95% Prediction Interval (PI) of the estimate, respectively. The number of scans for which the respective follow-up scan falls ‘within tolerance’ of the prediction determines the accuracy performance of the model.

Each individual patient has a varying number of sequential measurements over differing time lengths. These sequence of measurements were partitioned into two subsets; a calibration (DC, i.e. training) and a validation (DV, i.e. test) data set, as proposed by Hawkins-Daarud et al. [30]. The calibration set was used to calibrate the model, whereas the validation set was used for validation of the calibrated model. Apart from the initial scans, all scans in the population were incrementally and sequentially employed in validation to demonstrate whether our model predictions were consistent with the maximum diameter measured experimentally. As an example, let us say we have a patient with six consecutive scans and want to predict the maximum diameter at the 4th scan. Then, the known data set is $DC=\{t_1, t_2, t_3\}$ and the “true” diameter to be predicted is $DV=t_4$, in other words, the DV is the ground truth for the QoI. The performance of the predictive model at each particular QoI was assessed independently, because an acceptable performance at a specific QoI does not necessarily imply reasonable performance for all possible QoI.

All model parameters are encapsulated in the vector $\theta = (\theta_1, \theta_2, \dots, \theta_d) \in R^d$ and this is treated as a vector of random variables $\theta: \Omega \rightarrow R^d$, where Ω denotes a suitable sample space. This vector is estimated numerically (using MCMC) thus calibrating the exponential AAA growth model, given in Eq. (1), against a subset of the experimental data.

2.3.1. Calibration model—We use a Bayesian approach and follow the notation and terminology introduced by Gelman et al. [31]. The set of calibration parameters is denoted by the aforementioned θ , and the observed data are denoted by $y = \{y_1, y_2, \dots, y_n\}$.

Furthermore, the marginal and conditional probability of the density function (pdf) were denoted by $p(\cdot)$ and $p(\cdot/\cdot)$, respectively. In our AAA growth model, θ corresponds to the model parameters in Eq. (1) (i.e., $\theta_1 = \alpha$ and $\theta_2 = \beta$) and y corresponds to the maximum spherical diameter at the time points in the calibration data set SC. The observable outputs in the prediction model are related to the input parameters by

$$y = D(t; \theta, e) \quad (2)$$

where D and e respectively correspond to the maximum spherical diameter and the measurement error (the biological variability). The relationship between the maximum spherical diameters (observable outputs) and model inputs at time t can be formulated as

$$y = D(t; \theta) + \delta(t) + \varepsilon \quad (3)$$

where ε corresponds to error, the diameter $D(\cdot, \cdot)$ can be viewed as a function of t and $\theta(\alpha, \beta)$, and $\delta(t)$ corresponds to a discrepancy function. However, we ignored systematic model discrepancies explicitly by following the methodologies referred by Kennedy et al. [32], Higdon et al. [33] and Bayarri et al. [34]. As a result, a calibration model related to AAA growth outputs was given by;

$$y = D(t; \theta) + \varepsilon. \tag{4}$$

2.3.2. Bayesian inference and prediction

Statistical Model: The joint probability density function (pdf) denoted by $P_{JOINT}(\theta, y)$ can be defined as the product of the prior distribution of θ , denoted by $P_{PRIOR}(\theta)$ and the sampling distribution denoted by $P_{SAMPLE}(y|\theta)$ as follows;

$$P_{JOINT}(\theta, y) = P_{PRIOR}(\theta)P_{SAMPLE}(y|\theta). \tag{5}$$

The conditional probability assigned to the parameters, i.e. the posterior density, can be obtained by Bayes' theorem

$$P_{POST}(\theta|y) = P_{PRIOR}(\theta) \frac{P_{SAMPLE}(y \vee \theta)}{P_{PRIOR}^{PRED}(y)}, \tag{6}$$

where $P_{PRIOR}^{PRED}(y)$ denotes the marginal distribution, which is averaging the likelihood over all possible parameter values with respect to the prior density.

$$P_{PRIOR}^{PRED}(y) = \int P_{PRIOR}(\theta)P_{SAMPLE}(y|\theta)d\theta. \tag{7}$$

The density of $P_{SAMPLE}(y|\theta)$, a function of θ rather than y , is the likelihood function and interpreted as how likely a parameter value is, given a particular outcome. The subjective beliefs in the values of the parameters before the measurement are denoted by $P_{PRIOR}(\theta)$. Thus, a posterior distribution denoted by $P_{POST}(\theta|y)$ can be considered as an enhanced degree of belief, which is obtained with incorporation of experimental data.

Selection of the Prior Distribution: The posterior distribution of the population serves as the prior for both growth prediction models: Patient-Oriented Growth Prediction Model (POGPM) and Generalized Linear Model (GLM) enhanced POGPM. The methodology to find the Posterior Distribution of Population (PDoP) for a spherical diameter, which is used in POGPM, is explained here. The same approach was also followed to estimate the parameters for other significant geometrical parameters, which is used in GLM enhanced POGPM combined with a spherical diameter measurement.

The prior distributions of α and β are assumed to be normally distributed random variables with parameters (mean and deviation). The prior of α , the initial diameter at time $t=0$, was set at mean 30 mm because a AAA is clinically defined as an enlargement of the abdominal

aorta to >3.0 cm [1] and deviation 2 mm because the absolute intra-observer difference of the maximum diameter was 2 mm [35]. The prior of β (the growth rate) is set at mean 0.004 and variance 0.001 based on statistical characteristics of aneurysm growth [14]. Although the base distributions used in the common (population) model was Gaussian, Student's t-test distribution was used in the patient specific model because the number of observations for a single patient is too small to support a Gaussian. Student's t-distribution, on the other hand, can be applied as the POGPM since it is designed to be less concentrated around its peak and has heavier tails as the degree of freedom decreases, thus better capturing the level of uncertainty given less evidence, especially with respect to extreme observations. The more evidence we have per patient, the more this distribution will approximate a Gaussian.

The pre-assumed values for the mean of the prior distribution are updated using the Maximum A Posteriori (MAP) method based on the aforementioned data. A version of the Expectation-Maximization algorithm is used to find the most likely parameters; first, an initial growth curve, a function of α and β in Eq. (1), is chosen and patients' scans are time-shifted based on the measurements at the first observed scans. Then, the MAP estimate is made to update the predictors of the growth curve and to find a better fit function. The shifting and MAP estimation steps are iteratively repeated until the likelihood converges (i.e. total amount of error no longer decreases). As a result, the best fit of the growth curve, namely the "master curve", is found.

Selection of Likelihood: The likelihood function for the parameter θ , given data y , determines how the biological AAA growth model and experimental data y inform the posterior distribution. The measurement error of the maximum diameter at each time point was assumed to be independent and the processes determining the true diameter are deterministic. Furthermore, the experimental noise is assumed to be normally distributed about 0 (i.e. unbiased) with variance $\sigma_{D(t)}$, which denotes σ_D at time t .

Under these assumptions, the likelihood is formulated by

$$P_{SAMPLE}(y|\theta) = \prod_{i \in SC} \frac{1}{\sqrt{2\pi\sigma_V^2(t_i)}} \exp\left(\frac{-(y_i - D(t_i; \theta))^2}{2\sigma_V^2(t_i)}\right). \quad (10)$$

Sampling of Posterior Distribution: Obtaining the posterior distribution is analytically possible only when certain combinations of prior distribution and likelihood have been met; in general this is not the case. A numerical approach, using samples drawn from the posterior distribution $P_{POST}(\theta|y)$ via a discrete approximation is often required for this purpose. Hawkins-Daarud et al. [30] and Gelman et al. [31] proposed a solution to draw samples from the posterior distribution using a regular grid in the parameter space. However, this has a significant computational cost, especially for complex models having many inferred parameters. Instead, we applied a well-known method, Markov Chain Monte Carlo (MCMC) sampling, for posterior distribution in this study.

Probabilistic programming is an approach that uses automatic Bayesian inference on a user-defined probabilistic model with the help of MCMC sampling, and is therefore used to

perform inference and parameter estimation on arbitrarily complex probabilistic graphical models. The MCMC algorithm used is the No-U-Turn Sampler (NUTS) algorithm [20]. PyMC3 [36], an open source probabilistic programming framework written in Python, was used in POGPM and GLM enhanced POGPM. PyMC3 was preferred as it is a commonly used framework, with good community support, featuring an optimized inference engine based on likelihood gradient convergence, as well as a number of common distributions, such as Beta, Gamma, Binomial and Categorical, where the values of the parameters determine the location, shape or scale of the randomly generated numbers depending on the specific parameterization of the distribution.

2.4. Patient-oriented Growth Prediction Model (POGPM)

The Bayesian method is applied to predicting patient-oriented growth, as summarized in Fig. 1. In this study, a two-step approach based on Bayesian calibration [24] was used and the aneurysm growth model was specified according to individual patient characteristics.

The parameters of PDoP were estimated based on the spherical diameter using the whole population. The POGPM is specified, in contrast, based on each patient individually, as each patient has varying characteristics and growth rate. The posterior distribution from the population model (i.e. common for the subset of Korean patients) was set and fed to POGPM as the prior for each patient's specific model by using the Bayesian two-step model [24]. Once a patient specific model is built, the prediction of a measurement at any future time-point can be made, along with an estimate of the uncertainty associated with the prediction.

2.5. Generalized Linear Model (GLM) enhanced POGPM

Although, the POGPM can accurately predict follow-up diameter in the majority of cases, in some scans, sudden increases or decreases were observed. The commonalities between these scans were analyzed. First, all the scans were categorized based on their baseline spherical diameter into three classes, namely 'over-estimated', 'under-estimated' and 'within tolerance'. Then, all geometrical measurements belonging to the three groups were analyzed separately using pairwise t-tests to reveal if there was a significant predictor for sudden diameter growth. A p-value less than 0.05 was considered statistically significant.

In addition to spherical diameter, the study was extended using the GLM with Bayesian inference to take such significant features into account. Each pair of geometrical properties was analyzed in terms of their correlations and if two features were highly correlated ($\text{corr} > 0.9$), one of the two was dropped, because features with high correlation have almost the same effect on the dependent variable. For example, perimeter is strongly correlated with diameter ($\text{corr}=0.93$) and was removed from the feature set. Furthermore, the optimal model was built with only statistically significant variables ($p < 0.05$). Different features were removed and p-values in each case were measured in order to decide whether to keep a feature or not. Thus, additional candidate geometrical measurements, denoted by *CAN*, were selected based on p-values using Backward Elimination.

$$Growth X_1 MAX_{DIA_S} + X_k CAN, \quad (11a)$$

where CAN is an additional candidate geometrical measurement. The growth is a function of the posterior distribution of both spherical diameter (MAX_{DIA_S}) and CAN while X_k are the coefficients. The PDoP for CAN was found by following the same approach, as already explained, to find PDoP for MAX_{DIA_S} . The parameters of the population (mean and standard deviation), unknown parameters in Eq. (11), were then found using the GLM model, and were set as priors. These PDoPs, which were already specified for MAX_{DIA_S} and CAN according to observations made on the CT scans belonging to a particular patient, were used to subsequently predict aneurysm follow-up diameter based on time.

3. RESULTS

3.1. Posterior distribution of population (PDoP)

The Bayesian inference explained in the previous section was used to estimate the parameters of PDoP for 25 AAA patients using the exponential function. This will serve as prior to a distribution of predictors.

The estimated parameters of population posterior distribution using spherical diameter are demonstrated in Fig. 2. There are two parameters being estimated: the baseline diameter α (mean=32.06 mm, standard deviation=0.55 mm) and exponent of the growth rate β (mean=0.0043, standard deviation=0.0002). The parameters of the growth prediction model, α and β , are specified based on this fit.

The characteristics of the population growth were analyzed using different distributions such as z-score and Student's t-test. The posterior distributions of the stochastic values were virtually the same for both Gaussian and t-distributions because the number of samples ($n=106$) is sufficient that the t-distribution ($\alpha \sim N(31.9, 0.54)$, $\beta \sim N(0.0043, 0.0002)$) approximates the normal distribution ($\alpha \sim N(32.06, 0.55)$, $\beta \sim N(0.0043, 0.0002)$). Fig. 3 represents the normal distribution of the samples drawn from the specified model. The average and standard deviation of the follow-up diameter for the population is 43.41 mm and 7.05 mm.

The PDoP provides a growth model of two predictor variables; α and β were normally distributed random variables with parameters ($\alpha \sim N(32.063, 0.5498)$; $\beta \sim N(0.0043, 0.0002)$) respectively. Based on the mean of posterior distribution, aneurysm growth for the next diameter at any time can be predicted by Eq. (11) and Eq. (12):

$$T = \ln(D^{baseline} \div 32.063) \div 0.0043, \quad (11b)$$

$$D^{follow-up} = 32.063 * e^{(0.0043 * (t + T))}, \quad (12)$$

where $D^{baseline}$ describes the diameter at the baseline scan, T represents how many months have passed once the aneurysm was observed and t determines the period of time in months for the next prediction.

Figure 4 shows that the follow-up diameter was predicted within 2.7 mm error in 64 of 81 scans (79%) using the PDoP based on a 95% prediction interval. However, 17 of 81 scans (21%) did not follow the common properties of the population. The number of CT scans for which the growth rates are over- and under-estimated are 4/81 (5%) and 13/81 (16%) respectively.

3.2. Patient-oriented prediction of AAA growth

An individual POGPM was specified according to the patient specific growth characteristics. Figure 5 shows examples of a POGPM constructed for Patient 11 and Patient 23, using the consecutive scans of each as incremental observations, and the posterior distribution of the parameters for the whole population (i.e. using the PDoP) as a prior, as per the workflow of POGPM (Fig. 1).

The mean, standard deviation and the degree of freedom of the posterior distribution (estimated parameters of student-t distribution) at the 77th month were 43.72 mm, 0.47 mm and 1.81, respectively. Similarly, all these parameters of the distribution were estimated from the 4th scan observed, and both blue and orange lines were drawn in order to represent the upper and lower limit of the next prediction with respect to time. In this example, the observed diameter of Patient 11 at the 4th scan is 43.34 mm. The predicted diameters were between 43.05 and 44.39 mm with 0.68 confidence ($p=0.32$) and 41.50 and 45.94 mm with 0.95 confidence ($p=0.05$). The figure also shows that the last CT scan of the patient was outside of the prediction range with 0.68 confidence. However, the growth model would be updated using the observation for the 4th and 5th CT scans and the prediction range would be changed accordingly. This is an example of successful model construction according to the patients first 3 observed scans, because the observed diameter was found inside the limit of prediction range with both 0.68 and 0.95 confidence levels.

The growth model using diameter provided different results for posterior distributions specified by the characteristics of patient and population as Table 3 shows. The percentages of observed scans, accurately modeled in population and patient oriented growth, are respectively 79% ($n=64$) and 83% ($n=67$) specified with .95 confidences ($p=0.05$). The average errors were ± 2.67 mm and ± 2.61 mm respectively. Furthermore, 60 of 68 (88%) and 6 of 8 (75%) of scans were accurately predicted by POGPM in the 1st and 2nd years, respectively.

3.3. Enhanced prediction of AAA growth with morphological characteristics

The aneurysm growth could not be successfully modeled for some scans using only diameter. For example, the diameter of Patient 23 at the 3rd scan, was predicted between 39.13 and 44.1 mm with prediction intervals of 0.95 as demonstrated by Fig. 5. However, the observed diameter was 45.02 mm. Thus, the other geometric measurements were considered to help explain such unexpected change in the growth and to decrease the number of such inaccurate observations.

The common properties of the baseline scans were analyzed by taking all other geometrical measurements into account. The means and standard deviations of each category (under-estimated, over-estimated and within tolerance scans) are summarized in Table 2. The inter-

variance between categories was analyzed using the t-test (two tailed, equal variance) and the tortuosity of centerline was found significant ($p=0.0002$) for the categories of underestimated and within tolerance scans. In the GLM enhanced POGPM for Eq. 11, PAR is replaced by the parameter, $TORT_CL$.

Therefore, aneurysm growth was also modeled by considering the tortuosity of the centerline, in addition to diameter, using GLM enhanced POGPM. 86% ($n=70$) of observed scans were accurately modeled in GLM enhanced POGPM with .95 confidence intervals ($p=0.05$), and the average error was ± 2.79 mm as shown in Table 3. Furthermore, 93% and 75% of scans were accurately predicted by GLM enhanced POGPM in the 1st and 2nd years, respectively. The estimated parameters of posterior normal distribution of predictors and coefficients are as follows;

$$\begin{aligned} &\alpha_{DIAS} \sim \eta(32.063, 0.549), \beta_{DIAS} \sim \eta(0.0043, 0.0002), \alpha_{TORTCL} \sim \eta(1.012, 0.0047), \beta_{TORTCL} \sim \\ &\eta(0.0013, 0.00005), \\ &\theta_1 \sim \eta(1.023, 0.039), \theta_2 \sim \eta(-0.313, 1.532), \sigma \sim \eta(0.0, 1.0), \mu = \theta_1 * MAX_{DIAS} + \theta_2 * TORTCL, \\ &\text{and } Y \sim \eta(\mu, \sigma^2). \end{aligned}$$

4. DISCUSSION

In this study we developed an enhanced growth prediction model applicable to AAA growth, using Bayesian inference. An exponential growth model, commonly demonstrated in previous studies, was selected and the parameters for the posterior distributions were estimated from observations (scans). We used 106 CT scans from a 25 patient dataset to construct PDoP and further predicts patient-specific AAA growth. Thus, the prediction of a measurement at any time-point can be made, along with an evaluation of the associated uncertainty.

Follow-up diameters can be determined if a patient follows the common growth model of the population. However, this is not true for all scans belonging to the same patient. For example, 23% ($n=3$) of previously underestimated scans ($n=13$), were accurately modeled within tolerance, if the POGPM was specified according to individual characteristics, while their errors in millimeters were almost the same. The characteristic of an individual are important aspects for AAA patient management, because, for example, a slow growing AAA would not require frequent monitoring, whereas the opposite is true for a fast growing AAA. Therefore, Lee et al. [21] applied machine learning techniques for accurate prediction of AAA growth in an individual.

A patient-specific modeling of an AAA growth is an important step in terms of individualized diagnosis and clinical treatment. Zeinali-Davarani et al. used 3D geometry constructed from medical images and developed a computational framework for modeling AAA G&R [19]. In most studies of AAA biomechanics, the influence of the surrounding tissues was ignored [18]. This study, therefore, focused on further improvement of the G&R computational framework account for mechanical interaction between AAA and spine[18]. In addition to the prediction of an AAA, Zhang et al. also applied Bayesian calibration

method to G&R computational model to quantify the associated uncertainty in the prediction [37].

One of the main strengths of this study is to have a relatively large number of scans analyzed. Although there exist previous papers using a physics-based computational modeling approaches for predicting AAA growth [18][19] and a study associated with uncertainty [37], the number of real observations was relatively small and no such assessment of the prediction model accuracy was available in their comparisons. Therefore, the results of our proposed solution could not be directly compared with these results, even though their approaches have similar advantages as Table 4, the state of the art comparison, shows.

The morphology of aneurysms has also been found to play an important role, affecting the rate of growth and risk of rupture [8][9][38][39]. Among the total number of features (n=28); sac length, sac height, volume and surface area were found to be the highest indices from the feature selection algorithm, and the risk assessment of an AAA should be based on the accurate quantification of aneurysm sac and shape [22]. Similarly, Parikh et al. [23] implemented a decision tree algorithm to find the three most significant indices: AAA centerline length, L2-norm of Gaussian curvature and AAA wall surface area. These studies developed a model using a machine learning algorithm that is capable of discriminating whether an AAA requires elective or emergent intervention with high accuracy. In this study, the common properties of AAA scans with sudden aneurysm growth were also analyzed to see if there were significant ($p < 0.05$) predictors of sudden growth. The tortuosity of centerline was found to be significant ($p=0.0002$) for the categories of under-estimated and within tolerance scans, which might be a main factor behind such sudden growth. Our study corroborates the findings [23][24], which shows the importance of the aneurysm centerline in evolution of an AAA. Additionally, we developed a model based on probabilistic programming and predicted the growth rate at any time for better management of an AAA during the surveillance period rather than a classification.

Generalized Linear Model (GLM) enhanced POGPM was also used to take the tortuosity of centerline into account in the growth model and decrease the number of incorrect predictions due to cases of sudden growth. The percentage of observed scans that the diameter growth was over- and under-estimated were 5% (n=4) and 9% (n=7) respectively in GLM enhanced POGPM. 3 of 7 under-estimated scans were recorded at distant periods of time at 32, 54 and 56 months, which is not clinically routine during the surveillance period because the rescreening interval of almost more than 3 years is too long. The accuracy would be increased if these scans were discarded, but nevertheless chose to keep them. 30% (n=6) of previously overestimated scans (n=13) using POGPM were accurately modeled within tolerance, whereas there is no performance improvement observed in the under-estimated scans. Additionally, the average error (in millimeters) in GLM enhanced POGPM was almost the same as the others.

Time interval between consecutive scans affects the accuracy of the growth prediction model. For example, the aforementioned Lee et al. predicted the individual's AAA diameter in 85% and 71% of patients at 12 and 24 months follow-up, respectively [12]. Time interval

between consecutive scans, from 6 to 56 months, is not consistent in this study. Therefore, we categorized the scans based on the time intervals, namely, 1st and 2nd year. 88% and 93% of the scans are predicted using POGPM and GLM enhanced POGPM, respectively, within the 1st year (n=68). Both prediction models thus offer reasonable accuracy. However, their accuracy becomes 75% if the scans are recorded at 2nd year (n=8).

An alternative approach to make a diameter prediction for future AAA growth in an individual patient is to do a classification via a supervised machine learning technique. Shum et al. [22] developed a model on a retrospective study of 10 ruptured and 66 unruptured aneurysms using a decision tree algorithm and 87% of dataset were correctly classified. Similarly, Parikh et al. built a decision tree based on 150 AAA patients (75 electives and 75 emergent repaired) and demonstrated the classification accuracy of 81% [23]. They derived similar number of geometrical measurements from 3D constructed of an AAA (n=25 and n=31) as we have (n=21) and provide preferable results. The weakness of these approaches is, however, that they output a binary classification predicting the future state of the AAA as a categorical value rather than a numerical value.

UK Small Aneurysm Trial (UKSAT) [40] showed that the probability of exceeding 55 mm for small aneurysms is less than 1%, and annual, or less frequent, surveillance intervals are safe for all AAAs less than 45 mm. In other studies, the rupture risk for an AAA of 4–4.9 cm-diameter has been estimated to be 0.6–2.1% per year [41]. We also found that aneurysms of 4.5 and 4.9 cm are estimated to reach surgical size in 3 and 2 years, respectively (CI=0.95). This result was supported by the ADAM study, in which 27% of 4–5.5 cm-AAA randomized to the surveillance group had undergone surgical exclusion at 2 years' follow-up [41]. Similarly, AAAs of 4.5–4.9 cm-diameter are expected to reach surgical size in 2–3 years [42].

To avoid the computational inefficiency of a random walk and the requirement to tune the proposal distribution, especially given the high-dimensional target distribution in question, we decided on the Hamiltonian Monte Carlo (HMC) algorithm (or Hybrid Monte Carlo) [20], which is a Markov Chain Monte Carlo method for obtaining a sequence of random samples. We have not reported the complexity of the proposed solution to classify algorithms with respect to their run time or memory space requirements using Big-O notation. The main reason is that the algorithm does not take a very long time and requires a large memory requirement. Additionally, the HMC algorithm is a stochastic algorithm which is run with a pre-determined burn-in and subsequent fixed number of iterations [20].

A rapid expansion of AAA, often associated with higher rupture risk, might be observed. This is clinically important for the prognosis of aneurysm growth during surveillance because the required immediate intervention based on the criteria defined by international guidelines might be overlooked. Therefore, the aneurysm growth model was specified according to individual patient characteristics. Additionally, using other geometrical measurements enhanced the exponential growth model. A tool with the improved potential of predicting AAA expansion or assessment of rupture risk, which is important in terms of elective surgical intervention and patient management, was developed.

LIMITATIONS

Although this study has been able to provide a tool with the improved potential of predicting AAA expansion in order to help assessment of rupture risk, it has some limitations. First, this is a retrospective study, in which 106 CT scan images from 25 Korean AAA patients were obtained from a single center. The prediction model was specified based on the characteristics of a subset of a Korean population. However, it is known that the average annual growth rates based on baseline diameter have large variation [5], because various populations were examined [15]. Therefore, a new set of measurements in a large multicenter study can enhance the prediction capability of the model and contribute to the current method of surveillance of patients with small AAAs. The proposed solution would be applicable to any population for surgical planning and patient management. In addition to the morphology of an aneurysm, the individual genotypes [43] and environmental and demographic features of patients such as gender, a history of tobacco use, comorbidities and medications, which are important in aneurysm growth rate [7][43][44] but were out of the scope of this study. Furthermore, since the intra- and inter-observer variability in CT measurements is usually ± 5 mm, recognizing an aneurysm with a growth rate of 2 mm/year takes 3 years [3]. Even given these limitations, this study provides a clinically helpful tool for the management of AAA development by considering patient specific characteristics and various geometrical measurements, and offers an acceptable growth model for the development of an improved surveillance program, even for AAAs with sudden growth.

CONCLUSIONS

The proposed probabilistic growth model, which enhances the prediction of AAA expansion at any future time-point, can have important implications in elective surgical planning and patient management during surveillance. This study highlights the utility of such a prediction model built on patient individual characteristics and various geometrical measurements as a predictor for AAA growth, and the value of probabilistic programming techniques in the new era of precision medicine.

Acknowledgement

This work has been supported in part by the National Heart, Lung, and Blood Institute of the National Institutes of Health (R01HL115185 and R21HL113857).

REFERENCES

- [1]. Chaikof EL, Dalman RL, Eskandari MK, Jackson BM, Lee WA, Mansour MA, ... Starnes BW, "The Society for Vascular Surgery practice guidelines on the care of patients with an abdominal aortic aneurysm," *J. Vasc. Surg.*, vol. 67, no. 1, pp. 2–77, 2018. [PubMed: 29268916]
- [2]. Scott RAP, Ashton HA, Buxton MJ, Day NE, Kim LG, Marteau TM, ... Walker NM, "The Multicentre Aneurysm Screening Study (MASS) into the effect of abdominal aortic aneurysm screening on mortality in men: a randomised controlled trial," *Lancet*, vol. 360, no. 9345, pp. 1531–1539, 2002. [PubMed: 12443589]
- [3]. Limet R, Sakalihassan N, and Albert A, "Determination of the expansion rate and incidence of rupture of abdominal aortic aneurysms.," *J. Vasc. Surg.*, vol. 14, no. 4, p. 540, 1991. [PubMed: 1920652]

- [4]. Martufi G, Auer M, Roy J, Swedenborg J, Sakalihan N, Panuccio G, Gasser TC, and Christian T, "Multidimensional growth measurements of abdominal aortic aneurysms," *J. Vasc. Surg.*, vol. 58, no. 3, pp. 748–755, 2013. [PubMed: 23611712]
- [5]. Gharahi H, Zambrano BA, Lim C, Choi J, Lee W, and Baek S, "On growth measurements of abdominal aortic aneurysms using maximally inscribed spheres," *Med. Eng. Phys.*, vol. 37, no. 7, pp. 683–691, 2015, doi: 10.1016/j.medengphy.2015.04.011. [PubMed: 26004506]
- [6]. Novak K, Polzer S, Krivka T, Vlachovsky R, Staffa R, Kubicek L, Lambert L, and Bursa J, "Correlation between transversal and orthogonal maximal diameters of abdominal aortic aneurysms and alternative rupture risk predictors," *Comput. Biol. Med.*, vol. 83, pp. 151–156, 2017, doi: 10.1016/j.compbiomed.2017.03.005. [PubMed: 28282590]
- [7]. Brown PM, Zelt DT, and Sobolev B, "The risk of rupture in untreated aneurysms: the impact of size, gender, and expansion rate," *J. Vasc. Surg.*, vol. 37, no. 2, pp. 280–284, 2003. [PubMed: 12563196]
- [8]. Parr A, McCann M, Bradshaw B, Shahzad A, Buttner P, and Golledge J, "Thrombus volume is associated with cardiovascular events and aneurysm growth in patients who have abdominal aortic aneurysms," *J. Vasc. Surg.*, vol. 53, no. 1, pp. 28–35, 2011. [PubMed: 20934838]
- [9]. Lee K, Johnson RK, Yin Y, Wahle A, Olszewski ME, Scholz TD, and Sonka M, "Three-dimensional thrombus segmentation in abdominal aortic aneurysms using graph search based on a triangular mesh," *Comput. Biol. Med.*, vol. 40, no. 3, pp. 271–278, 3 2010, doi: 10.1016/J.COMPBIOMED.2009.12.002. [PubMed: 20074719]
- [10]. Scotti CM, Shkolnik AD, Muluk SC, and Finol EA, "Fluid-structure interaction in abdominal aortic aneurysms: effects of asymmetry and wall thickness," *Biomed. Eng. Online*, vol. 4, no. 1, p. 64, 2005. [PubMed: 16271141]
- [11]. Siika A, Liljeqvist ML, Hultgren R, Gasser C, and Roy J, "AAA Rupture Often Occurs Outside the Maximal Diameter Region and is Preceded by Rapid Local Growth and an Increased Biomechanical Rupture Risk Index," *Eur. J. Vasc. Endovasc. Surg.*, vol. 50, no. 3, p. 390, 2015.
- [12]. Lee R, Jones A, Cassimjee I, and Handa A, "International opinion on priorities in research for small abdominal aortic aneurysms and the potential path for research to impact clinical management," *Int. J. Cardiol.*, vol. 245, pp. 253–255, 2017. [PubMed: 28874296]
- [13]. Kurvers H, Veith FJ, Lipsitz EC, Ohki T, Gargiulo NJ, Cayne NS, ... Santiago C, "Discontinuous, staccato growth of abdominal aortic aneurysms," *J. Am. Coll. Surg.*, vol. 199, no. 5, pp. 709–715, 2004, doi: 10.1016/j.jamcollsurg.2004.07.031. [PubMed: 15501110]
- [14]. Akkoyun E, Gharahi H, Kwon ST, Zambrano BA, Rao A, Acar AA, Lee W, and Baek S, "Defining master curve of abdominal aortic aneurysm growth and its potential utility of clinical management," *Manuscript Submitted Publication*, 2019.
- [15]. Powell JT, Sweeting MJ, Brown LC, Gotensparre SM, Fowkes FG, and Thompson SG, "Systematic review and meta-analysis of growth rates of small abdominal aortic aneurysms," *Br. J. Surg.*, vol. 98, no. 5, pp. 609–618, 2011. [PubMed: 21412998]
- [16]. Forsythe RO, Newby DE, and Robson JMJ, "Monitoring the biological activity of abdominal aortic aneurysms beyond ultrasound," *Heart*, vol. 102, no. 11, pp. 817–824, 2016. [PubMed: 26879242]
- [17]. Abbas A, Attia R, Smith A, and Waltham M, "Can We Predict Abdominal Aortic Aneurysm (AAA) Progression and Rupture by Non-Invasive Imaging? A Systematic Review," *Int. J. Clin. Med.*, vol. 2, no. 04, p. 484, 2011.
- [18]. Farsad M, Zeinali-Davarani S, Choi J, and Baek S, "Computational Growth and Remodeling of Abdominal Aortic Aneurysms Constrained by the Spine.," *J. Biomech. Eng.*, vol. 137, no. 9, 9 2015, doi: 10.1115/1.4031019.
- [19]. Zeinali-Davarani S and Baek S, "Medical image-based simulation of abdominal aortic aneurysm growth," *Mech. Res. Commun.*, vol. 42, pp. 107–117, 2012, doi: 10.1016/j.mechrescom.2012.01.008.
- [20]. Hoffman MD and Gelman A, "The No-U-Turn sampler: adaptively setting path lengths in Hamiltonian Monte Carlo.," *J. Mach. Learn. Res.*, vol. 15, no. 1, pp. 1593–1623, 2014.

- [21]. Lee R, Jarchi D, Perera R, Jones A, Cassimjee I, Handa A, ... Sideso E, "Applied machine learning for the prediction of growth of abdominal aortic aneurysm in humans," *EJVES short reports*, vol. 39, pp. 24–28, 2018. [PubMed: 29988820]
- [22]. Shum J, Martufi G, Martino ED, Washington CB, Grisafi J, Muluk SC, and Finol EA, "Quantitative assessment of abdominal aortic aneurysm geometry," *Ann. Biomed. Eng.*, vol. 39, no. 1, pp. 277–286, Jan. 2011, doi: 10.1007/s10439-010-0175-3. [PubMed: 20890661]
- [23]. Parikh SA, Gomez R, Thirugnanasambandam M, Chauhan SS, De Oliveira V, Muluk SC, Eskandari MK, and Finol EA, "Decision Tree Based Classification of Abdominal Aortic Aneurysms Using Geometry Quantification Measures," *Ann. Biomed. Eng.*, vol. 46, no. 12, pp. 2135–2147, Dec. 2018, doi: 10.1007/s10439-018-02116-w. [PubMed: 30132212]
- [24]. Spyroglou II and Rigas AG, "A two-step Bayesian approach for modeling a complex neurophysiological system," *International journal of biology and biomedical engineering*, vol. 12, pp. 66–74, 2018.
- [25]. Glickman ME and Van Dyk DA, "Basic bayesian methods," in *Topics in Biostatistics*, Springer, 2007, pp. 319–338.
- [26]. Bolstad WM, *Understanding computational Bayesian statistics*, vol. 644 John Wiley & Sons, 2009.
- [27]. Dunson DB, "Commentary: practical advantages of Bayesian analysis of epidemiologic data," *Am. J. Epidemiol.*, vol. 153, no. 12, pp. 1222–1226, 2001. [PubMed: 11415958]
- [28]. Bergamaschi R, Berzuini C, Romani A, and Cosi V, "Predicting secondary progression in relapsing--remitting multiple sclerosis: a Bayesian analysis," *J. Neurol. Sci.*, vol. 189, no. 1–2, pp. 13–21, 2001. [PubMed: 11535229]
- [29]. Forrester ML, Pettitt AN, and Gibson GJ, "Bayesian inference of hospital-acquired infectious diseases and control measures given imperfect surveillance data," *Biostatistics*, vol. 8, no. 2, pp. 383–401, 2006. [PubMed: 16926230]
- [30]. Hawkins-Daarud A, Prudhomme S, van der Zee KG, and Oden JT, "Bayesian calibration, validation, and uncertainty quantification of diffuse interface models of tumor growth," *J. Math. Biol.*, vol. 67, no. 6–7, pp. 1457–1485, 2013. [PubMed: 23053536]
- [31]. Gelman A, Carlin JB, Stern HS, Dunson DB, Vehtari A, and Rubin DB, *Bayesian data analysis*, Chapman and Hall/CRC, 2013.
- [32]. Kennedy MC and O'Hagan A, "Bayesian calibration of computer models," *J. R. Stat. Soc. Ser. B (Statistical Methodology)*, vol. 63, no. 3, pp. 425–464, 2001.
- [33]. Higdon D, Kennedy M, Cavendish JC, Cafeo JA, and Ryne RD, "Combining field data and computer simulations for calibration and prediction," *SIAM J. Sci. Comput.*, vol. 26, no. 2, pp. 448–466, 2004.
- [34]. Bayarri MJ, Berger JO, Paulo R, Sacks J, Cafeo JA, ... Tu J, "A framework for validation of computer models," *Technometrics*, vol. 49, no. 2, pp. 138–154, 2007.
- [35]. Singh K, Jacobsen BK, Solberg S, Bønaa KH, Kumar S, Bajic R, and Arnesen E, "Intra-and interobserver variability in the measurements of abdominal aortic and common iliac artery diameter with computed tomography. The Tromsøstudy," *Eur. J. Vasc. Endovasc. Surg.*, vol. 25, no. 5, pp. 399–407, 2003. [PubMed: 12713777]
- [36]. Salvatier J, V Wiecki T, and Fonnesbeck C, "Probabilistic programming in Python using PyMC3," *PeerJ Comput. Sci.*, vol. 2, p. e55, 2016.
- [37]. Zhang L, Jiang Z, Choi J, Lim CY, Maiti T, and Baek S, "Patient-Specific Prediction of Abdominal Aortic Aneurysm Expansion using Bayesian Calibration," *IEEE J. Biomed. Heal. Informatics*, vol. 23, no. 6, pp. 2537–2550, 2019.
- [38]. Scotti CM, Shkolnik AD, Muluk SC, and Finol EA, "Fluid-structure interaction in abdominal aortic aneurysms: Effects of asymmetry and wall thickness," *Biomed. Eng. Online*, vol. 4, no. 1, pp. 64, 2005, doi: 10.1186/1475-925X-4-64. [PubMed: 16271141]
- [39]. Zambrano BA, Gharahi H, Lim CY, Jaber FA, Choi J, Lee W, and Baek S, "Association of Intraluminal Thrombus, Hemodynamic Forces, and Abdominal Aortic Aneurysm Expansion Using Longitudinal CT Images," *Ann. Biomed. Eng.*, vol. 44, no. 5, pp. 1502–1514, 2016, doi: 10.1007/s10439-015-1461-x. [PubMed: 26429788]

- [40]. United Kingdom Small Aneurysm Trial Participants, “Long-term outcomes of immediate repair compared with surveillance of small abdominal aortic aneurysms,” *N. Engl. J. Med.*, vol. 346, pp. 1445–1452, 2002. [PubMed: 12000814]
- [41]. Lederle FA, Wilson SE, Johnson GR, Reinke DB, Littooy FN, Acher CW, ... Bandyk D “Immediate repair compared with surveillance of small abdominal aortic aneurysms,” *N. Engl. J. Med.*, vol. 346, pp. 1437–1444, 2002. [PubMed: 12000813]
- [42]. Vega de Céniga M, Gómez R, Estallo L, Rodríguez L, Baquer M, and Barba A, “Growth rate and associated factors in small abdominal aortic aneurysms,” *Eur. J. Vasc. Endovasc. Surg.*, vol. 31, no. 3, pp. 231–236, 2006, doi: 10.1016/j.ejvs.2005.10.007. [PubMed: 16293428]
- [43]. Li J, Pan C, Zhang S, Spin JM, Deng A, Leung LLK, ... Snyder M, “Decoding the Genomics of Abdominal Aortic Aneurysm.,” *Cell*, vol. 174, no. 6, pp. 1361–1372.e10, 9 2018, doi: 10.1016/j.cell.2018.07.021. [PubMed: 30193110]
- [44]. Helderman F, Manoch IJ, Breeuwer U, Kose H, Boersma, Van Sambeek M, ... Krams R, “Predicting patient-specific expansion of abdominal aortic aneurysms,” *Eur. J. Vasc. Endovasc. Surg.*, vol. 40, no. 1, pp. 47–53, 2010. [PubMed: 20346709]

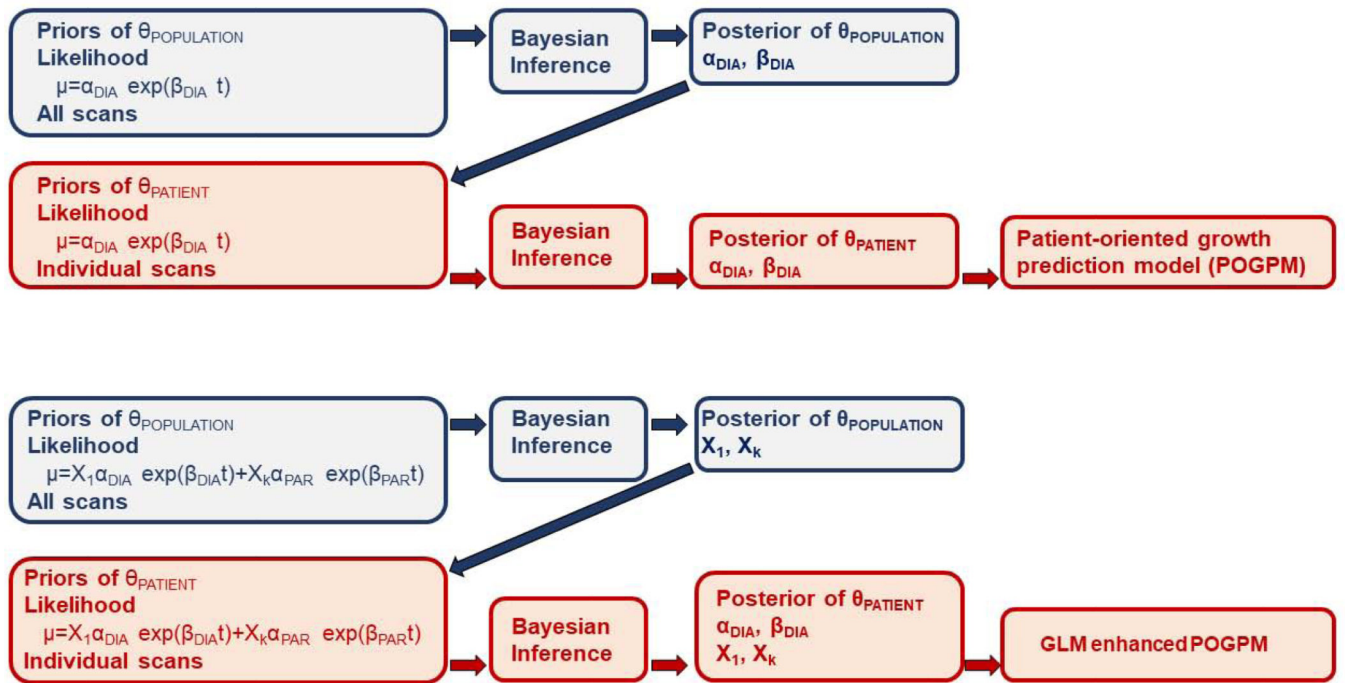


Figure 1. The work-flow diagrams for POGPM (top) and GLM enhanced POGPM (bottom).

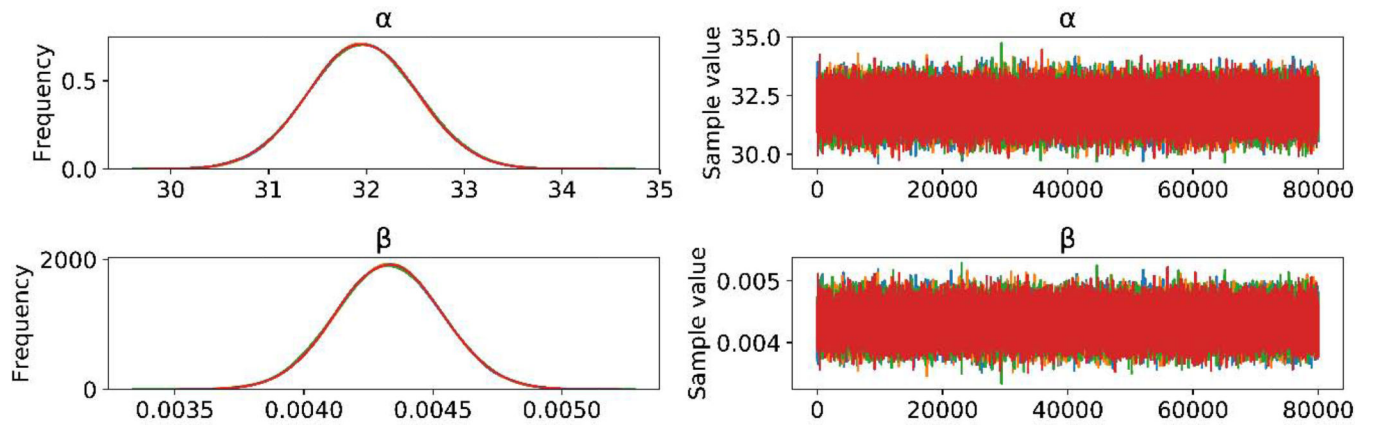


Figure 2.
The frequencies of estimated parameters for the PDoP growth model (α and β) and parameter values from drawn samples

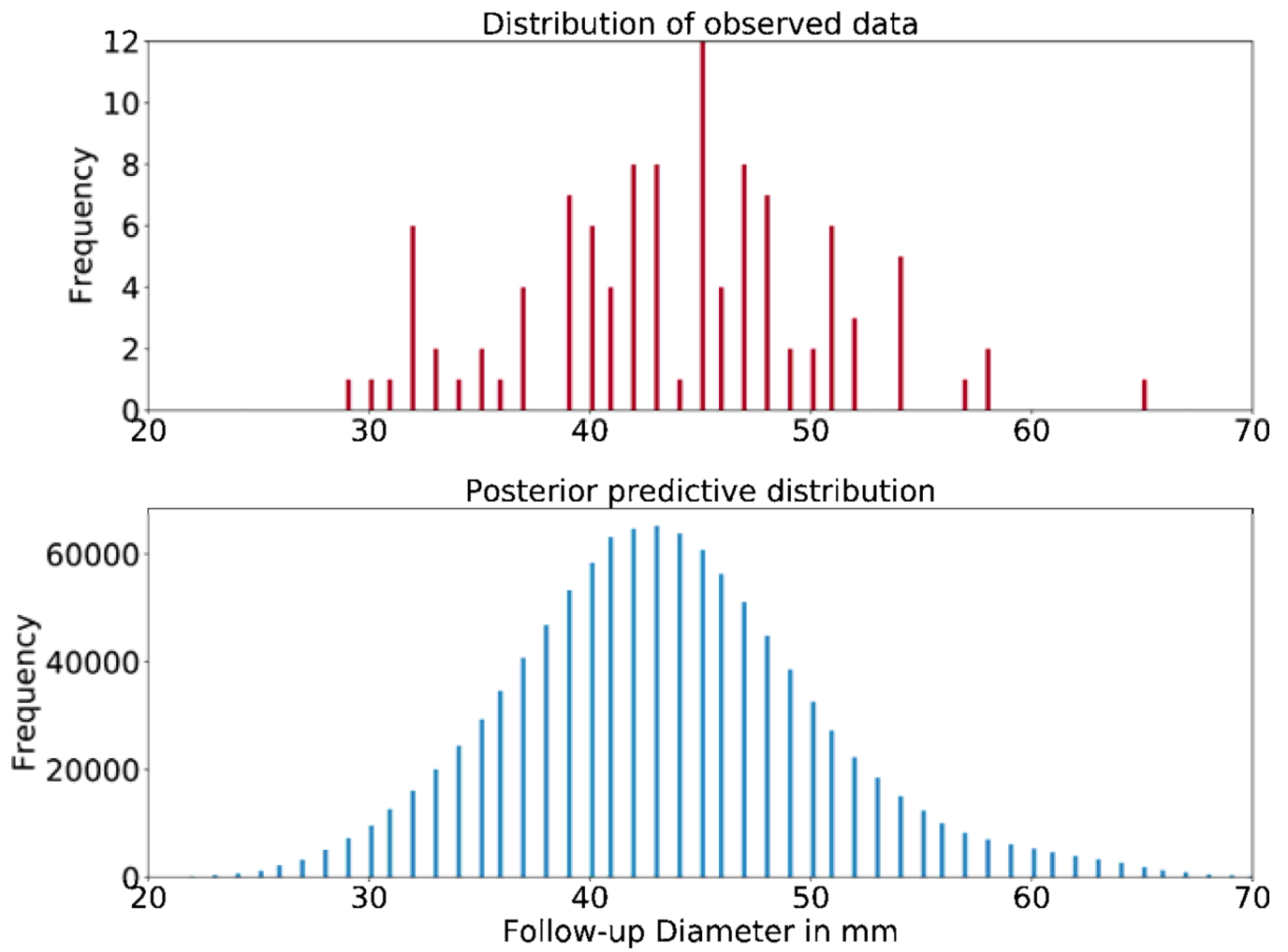


Figure 3. The distribution of observed scans (above) and the posterior distribution of the drawn samples for the Korean population (below)

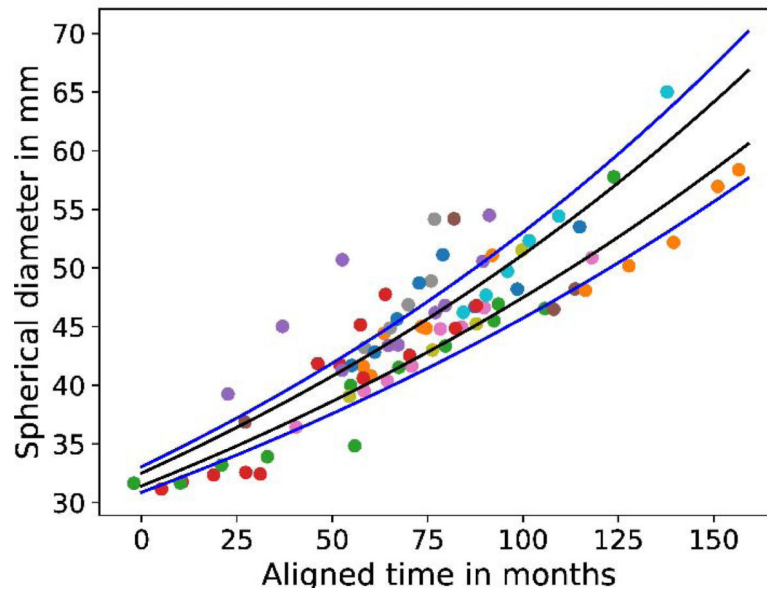


Figure 4.

The observed scans and aneurysm growth model based on the estimated parameters of PDoP and time interval between consecutive scans with 0.68 and 0.95 prediction interval. The aligned time is the shared time axis for all the patients. Since the AAA stages of the patients at the time of first scan were not the same, the time of the scan must be shifted in the shared time axis. The follow-up diameters of the 81 CT scans from 25 patients are marked on the plot with dots, where each color indicates an individual patient. Since the first scan of each patient was known, only follow-up scans (81 of 106 scans) that were QoIs in prediction, are presented in the graph.

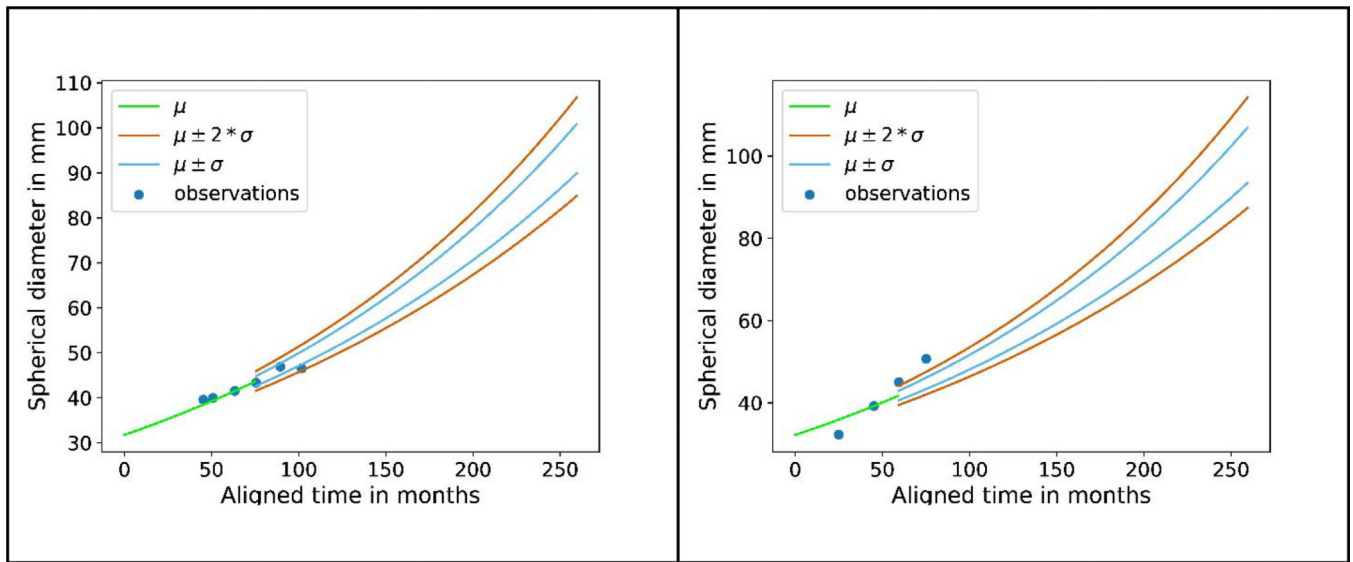


Figure 5. An example of the demonstration of the prediction capability of a POGPM at the 77th month (4th observed scans of patient with id 11) and at the 59th month (3rd observed scans of patient with id 23) with prediction intervals of 0.68 and 0.95. The time was aligned according to population growth curve. All previously obtained measurements for a patient were used for predicting the measurement at the next scan.

Table 1

The definitions of geometrical measurements

Measurement	Description
MAX _{DIA_S}	the maximum inscribed spherical diameter within an AAA in mm
MAX _{DIA_A} , MAX _{DIA_O}	the maximum axial and orthogonal diameter for the entire AAA in mm
MAX _{PER_A} , MAX _{PER_O}	the maximum perimeter for the entire AAA on axial and orthogonal planes in mm
DIA _{PER_A} , DIA _{PER_O}	the perimeter on axial and orthogonal planes at the maximum spherical diameter in mm
VOL _{AAA}	the total volume of the aneurysm in mm ³
VOL _{ILT}	the total volume of the thrombus in mm ³
VOL _{LUMEN}	the total volume of the lumen in mm ³
MIN _{DIA_A} , MIN _{DIA_O}	the minimum diameter throughout the AAA on axial and orthogonal planes in mm
MAX _{ECC_A} , MAX _{ECC_O}	the maximum eccentricity throughout the AAA on axial and orthogonal planes
DIA _{ECC_A} , DIA _{ECC_O}	the eccentricity on axial and orthogonal planes at the maximum spherical diameter
MAX _{ILT}	the maximum thrombus thickness for the entire AAA in mm
A _{ILT}	the AAA surface fraction of area covered by ILT content
TORT _{CL}	the ratio of the total centerline length to the length of the line joining the first and last point

Table 2

The mean and standard deviation of each category, and their paired t-test results.

		A _{ILT}	MAX _{ILT}	VOL _{LUMEN}	MAX _{ECC_O}	MIN _{DIA_O}	TORT _{CL}
Under-estimated Scans (U) n=10	mean	0.35	13.04	62019.15	1.40	17.92	1.19
	sd	0.22	4.00	16077.36	0.27	4.06	0.12
Over-estimated Scans (O) n=4	mean	0.26	10.50	59352.61	1.24	19.58	1.12
	sd	0.22	6.41	9093.67	0.04	2.35	0.05
Within Tolerance Scans (T) n=67	mean	0.30	13.92	61669.42	1.34	19.14	1.10
	sd	0.17	6.86	16930.94	0.23	2.96	0.06
T-Test Between Categories (p-values)	U-T	0.3747	0.6952	0.9513	0.4247	0.2511	0.0002
	T-O	0.6755	0.3357	0.7879	0.4112	0.7743	0.5114

Table 3.

The percentage of scans accurately modeled using PDoP, the POGPM and GLM enhanced POGPM

	Underestimated Scans	Overestimated Scans	Within Tolerance Scans	Error in mm
PDoP	16% (n=13)	5% (n=4)	79% (n=64)	2.67
POGPM	12% (n=10)	5% (n=4)	83% (n=67)	2.61
GLM enhanced POGPM	9% (n=7)	5% (n=4)	86% (n=70)	2.79

Author Manuscript

Author Manuscript

Author Manuscript

Author Manuscript

Table 4.

The state of the art comparison

Method	Motivation	Approach	Methods	Datasets	Uncertainty	Accuracy
Proposed model (POGPM)	prediction of future AAA growth	Two-stage Bayesian calibration	Probabilistic programming	106 CT scans	associated	83% of scans were predicted in 95% CI
Proposed model (GLM enhanced POGPM)	prediction of future AAA growth	Two-stage Bayesian calibration	Probabilistic programming	106 CT scans	associated	86% of scans were predicted in 95% CI
Farsad et al. (2015) [18]	trace to alteration of future AAA shape	G&R model	Finite Element Analysis	a few cases for demonstration	not capable	success demonstration on a few cases
Zeinali-Davarani et al. (2012) [19]	trace to alteration of future AAA shape	G&R model	Finite Element Analysis	a few cases for demonstration	not capable	success demonstration on a few cases
Zhang et al. (2019) [37]	trace to alteration of future AAA shape	Bayesian calibration and G&R model	Finite Element Analysis	a few cases for demonstration	associated	success demonstration on a few cases
Lee et al. (2018) [21]	prediction of future AAA growth	Machine learning	Non-linear Kernel support vector regression	94 patients	not capable	85% and 71% at 12 and 24 months
Shum et al. (2011) [22]	Classification (ruptured vs unruptured)	Machine learning	J48 decision tree algorithm	76 AAA patients	not capable	classification accuracy of 87%
Parikh et al. (2018) [23]	Classification (elective vs emergent AAA repair)	Machine learning	C5.0 decision tree	150 AAA patients	not capable	classification accuracy of 81%